Wavelets-based approach for online Fuel Cells Remaining Useful lifetime Prediction

Mona Ibrahim, Nadia Yousfi Steiner, Samir Jemei, Daniel Hissel

FEMTO-ST UMR CNRS 6174, FCLAB Research Federation FR CNRS 3539, University of Franche-Comte, rue Ernest Thierry Mieg, 90010 Belfort Cedex, France
Laboratory of Mathematics of Besancon, 16 route de Gray, 25000 Besancon
2 LABEX ACTION CNRS, FEMTO-ST UMR CNRS 6174
(mona.ibrahim, daniel.hissel, samir.jemei, nadia.steiner@univ-fcomte.fr)

***Abstract*— Prognostics and Health Management (PHM) techniques for Proton Exchange Membrane Fuel Cell (PEMFC) systems are of great importance for increasing their reliability and sustainability. PEMFC systems suffer from relatively poor long-term performance and durability, and prediction and prognosis can give early indications about when components should be fixed or replaced. Prognostics modelling needs to take account of a number of phenomena, including degradation mechanisms that are not easily measured. A number of works are currently investigating PHM in fuel cell systems, as well as the problem of estimating Remaining Useful Lifetime (RUL). Any reduction in the volume of data required for making predictions is clearly advantageous. In this work, a univariate prognostic approach based on signal processing, namely Discrete Wavelet Transform (DWT) is proposed. The proposed approach aims at achieving an online prognostic for PEMFC systems. DWT is first introduced, and then the predictions are built using the power signals of two different PEMFC stacks in two different scenarios, namely static and dynamic operating conditions. Results show that the method is reliable for online prediction of power, with prediction errors less than 3%.**

***Index Terms*— fuel cell prognostics, data-driven models, discrete wavelet transform, RUL prediction.**

I. INTRODUCTION

In recent years PEMFCs have been seen as an environmentally friendly technology because of their clean chemical reactions (they use hydrogen to produce electricity, heat and water), and their efficiency. They can replace internal combustion engines in vehicles [1][2]. Fuel cells (FCs) have the potential to provide heat and electricity not only for vehicles, but also for buildings, including houses. Unfortunately, in comparison to other technologies, they have low reliability and a short lifespan [3] [4].

The reliability of the PEMFC stack is improving over time, but like any device involving chemical, physical, and mechanical processes, the lifetime of PEMFCs may be shortened by a number of direct and indirect factors such as the deterioration of materials, imperfect cell/stack design and assembly, inadequate operating conditions, and impurities and contaminants in incoming gases. Although a loss of performance over time is unavoidable, the rate of degradation can be minimized through the use of effective diagnostic and prognostic tools that encapsulate an understanding of how and why degradation and failures occur. Diagnostic [5]-[7] and prognostic methodologies for assessing the state of health of a fuel cell and predicting its remaining lifetime need to be designed and implemented, to bring about an improvement in system performance.

Fuel cell system prognostics involve building a reliable model that is able to predict how the representative parameters for degradation and ageing of the FC will change, and that can estimate Remaining Useful Lifetime (RUL). Prognostics have several objectives: besides the aim of avoiding degradation and even catastrophic failures, there are the aims of extending FC lifetime and availability, optimizing service, minimizing risk and reducing costs. Approaches to prognosis can be separated into three broad groups: Model-based [8]-[12], data-driven [13]-[21] and hybrid approach [22].

Since fuel cell systems are complex, non-linear, multi-physics (fluidic, thermal, mechanical, and electro-chemical) and multi-scale (time, space) systems, with strong interaction between parameters belonging to different subsystems, it is difficult to develop complete, precise models of operation, degradation and ageing. For this reason, data-driven prognostics would appear easier to implement, since they do not require an a priori deep understanding of all the ageing mechanisms affecting the stack.

Javed et al. [23] have pointed out that data-driven approaches for estimating the RUL of a FC system can themselves be classified into two groups. The first group corresponds to univariate-degradation-based models and the second group corresponds to direct RUL prediction models.

Silva et al. [17] developed a data-driven approach that they called an Adaptive Neuro-Fuzzy Inference System (ANFIS), for PEMFC stack temperature prognostics, using data collected on the PEMFC stack.

In another work, Morando et al. [24] applied a data-driven approach, Echo State Network (ESN), for PEMFC stack prognostics.

In one recent paper [25] the authors developed an approach based on a particle filtering for estimating the RUL of PEMFC under two operating conditions: steady state and dynamic.

Finally, Javed et al [26] presented an approach for PEMFC stack prognostics using a constraint-based Summation-Wavelet Extreme Learning Machine.

The data-driven methods developed in the literature have two major problems. First, they all need a large amount of data for the learning phase (exogenous and past data). Second, they all need to be trained (learning from examples) to make predictions, which means that if new data become available (new examples), the models need to be rebuilt.

To help overcome these problems, in this paper we propose a new data-driven prognosis approach for PEMFC. The model is univariate: unlike multivariate approaches [26] that need exogenous data, our method does not take exogenous data into account, and predictions can be made using only past observations of the power signal (univariate time series), meaning that fewer data and acquisition devices are required.

The model uses the past values of this signal up to a defined time t and predicts new values up to a certain time t+h; thus, the process of degradation is predicted and an online prognosis can be made. The proposed approach is mainly based on Wavelet

Transform (WT), which has been widely used for fuel cell monitoring [27]-[32], as well as many other applications [33]-[35].

The advantage of WT, specifically of Discrete Wavelet Transform (DWT), is its ability to represent a given time series (or signal) with a small number of coefficients (the approximation coefficients), and consequently only a small quantity of data can be sufficient for performing a prediction. The proposed approach consists of considering the output signal of a PEMFC and decomposing a segment of 168 hours (one week) using DWT. The power signals considered in this article represent the data from two long-duration ageing tests of 1000 hours, and therefore they include the processes of degradation that will be considered in the present work.

After decomposition, a set of approximations coefficients (see section II) can be obtained and can represent the original signal with a smaller number of observations (168 hours represented by 21 hours). Predictions are made on this new set using mathematical regression models: Auto-Regressive Integrated Moving Average 'ARIMA' and polynomial regression. The prediction horizon is set to 21 hours. Once the prediction is made, inverse DWT is applied to create the approximation signal of 168 hours using the obtained prediction (see section II). These 168 hours represent the prediction of degradation, and will be compared with the actual signal in terms of the mean square error. Thereafter, this operation is repeated for the next 5 weeks in order to complete the online prognosis. The quantity of delivered power (with constant current) is an indicator of the RUL, since the performance of the considered PEMFC ceases to be satisfactory once the power drops by about 5.5% from the initial value (this value is given here as an example, and may be adapted according to the constraints of the application).

The novelty of the proposed approach is that unlike the approaches developed in the literature, it is a univariate model without a training part; that is, the model does not learn the relationship between the observations by training (as black box systems do, for example), but only by attributing a suitable analytical model. Moreover, a long-term prediction (168 hours) can be achieved by predicting only 21 hours using DWT and inverse DWT.

This paper is organized as follows: In section II the description of the wavelet transform and the model description are given and in section III the collection of experimental data is described. The analysis of results and discussion are detailed in section IV, and finally section V is a general conclusion of the present work.

II. PEMFC prognostics method: the mathematical framework

Discrete Wavelet Transform (DWT) is an effective method for non-stationary signal filtering and processing. DWT has been used in a variety of fields including medicine, energy management, image processing and computer vision. The greatest advantage of DWT is localization in both time and frequency [36]. However, signals used for prognostics (voltage, power, etc…) are also non-stationary, and so DWT would appear to be a suitable method for analyzing these signals too.

A. *Discrete wavelet transform*

Discrete Wavelet Transform (DWT) is a method commonly used in signal processing. Given a time series (or a signal) Y (t), DWT allows an analysis of Y (t) in different scales over time. A wavelet φ is an oscillating, well-localized function having a finite vanishing moment [36]-[38].

Using a function φ, with another wavelet ω, an orthogonal basis of L2 (the set of signals with finite energy) can be constructed (in this case, φ is termed the mother wavelet and ω the father wavelet).

Using these two functions, the wavelet basis is defined by:

$$WB = \{\varphi_{j,k}(t) = \varphi(2^{-j}t - k), \omega_{j,k}(t) = \omega(2^{-j}t - k)\ , j, k\ \in \mathbb{Z}\} \quad (1)$$

where k is the translation parameter (in time), j is the scale (an integer indicating how the wavelet is stretched or compressed; see Fig. 1).

The projection of the signal Y over the basis WB is called the discrete wavelet transform.

Choosing scale j, the DWT of Y can be written as follows:

$$Y(t) = \sum_{k\in\mathbb{Z}} 2^{-\frac{j}{2}} c_j(k)\varphi(2^{-j}t - k) + \sum_{i=1}^{j}\sum_{k\in\mathbb{Z}} 2^{-\frac{j}{2}} d_i(k)\omega(2^{-j}t - k) \quad (2)$$

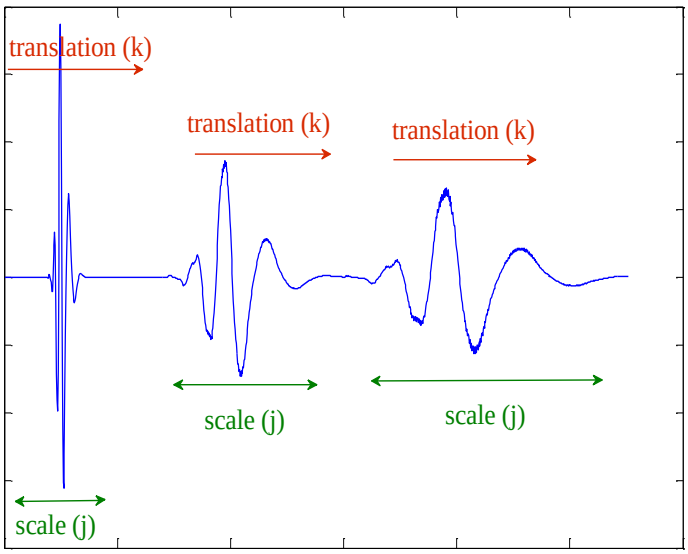

Fig. 1. Translation and scaling of the wavelet transform

The first series $c_j(k)$ is known as the approximation coefficients and can represent the trend of Y, while $d_i(k)$ are known as the detail coefficients. Let C be the set of the approximation coefficients $c_j(k)$.

Equation (2) includes two operations: a down sampling (data divided by 2) and a convolution over the whole time interval [39]. These characteristics are similar to a high pass and low pass filtering. Therefore, the wavelets (φ and ω) can be linked to low and high pass filters respectively [40].

For each level j, the length of the original signal is divided by 2 as a result of the down sampling, and therefore the length of the approximation coefficients is equal to the length of the original signal divided by 2^j .

The DWT consists of two steps: analysis (or decompositions) where the detail and approximation coefficients are obtained by the filtering processes, and synthesis (or reconstruction) where the coefficient sets can be represented by signals having the same length of the original signal Y, and are obtained by a up sampling and a convolution [40]. The process can be illustrated as shown in Fig. 2.

Inverse Discrete Wavelet Transform (IDWT) allows a reconstruction of the original signal using the set of approximation and detail coefficients, by an inverted operation of DWT.

It should be noted that the obtained signal A (signal constructed using the approximation coefficients) has the same shape as Y: in other words, it can describe the trend of Y,

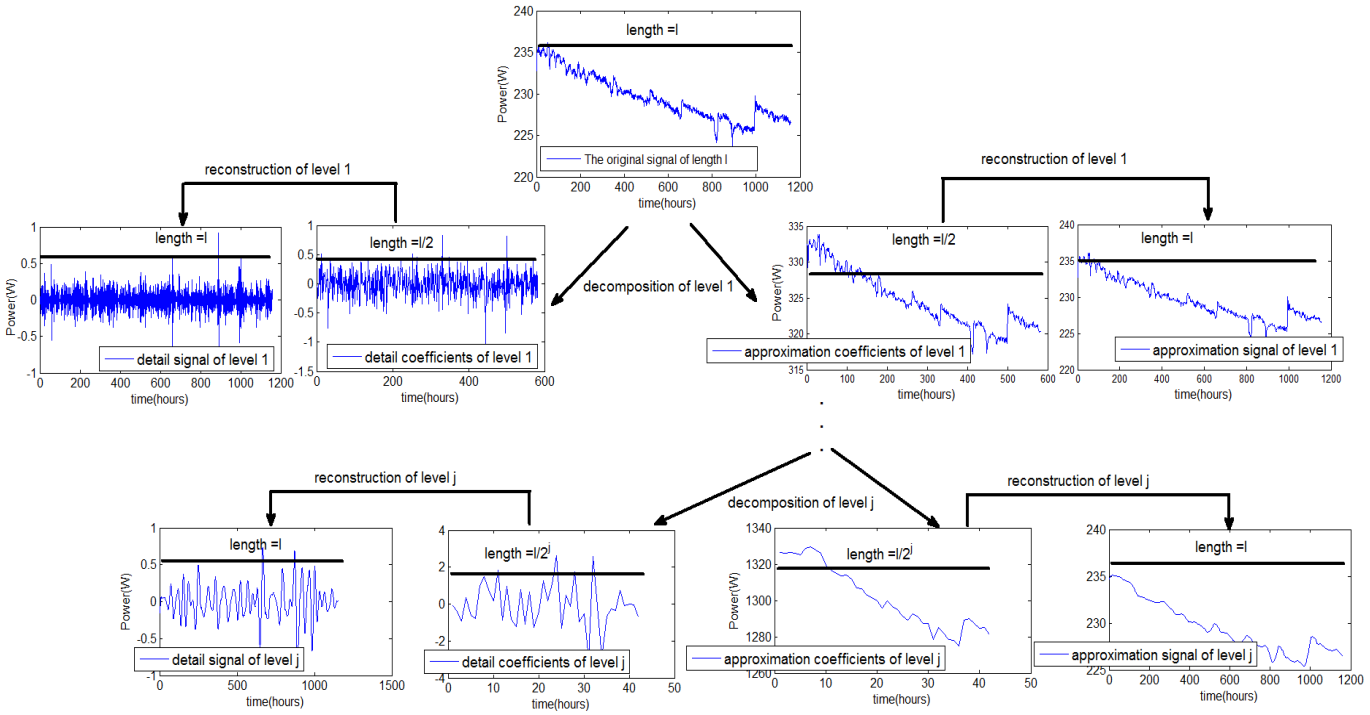

Fig. 2. The approximation coefficients and approximation signal obtained by DWT for a given time series.

without noises, and has the same length as Y.

B. Proposed PEMFC prognostic approach

The two fuel cell stacks considered in this study are from the same manufacturer and have the same initial characteristics. The first stack, FCd, was operated under dynamic current testing conditions, while the second stack, FCs, was operated in stationary regime under more or less nominal conditions. Both stacks were operated 24 hours a day over about 1000 hours.

The predictions were made using the power signals of both stacks FCd and FCs. The power was calculated using the formula:

$$P(t) = U(t).U(t) \qquad (3)$$

where U and I are respectively the given voltage and current of the stack.

The voltage and the current are functions of time; therefore, the power P is also a function of time and can be considered as a signal or time series. P (t) is the observation at time t.

As we saw above, by applying the DWT of level j, the original signal of length L can be divided into $j + 1$ sets: the set of approximation coefficients of length $L/2^j$ and j sets of detail coefficients.

It is important to note the difference between the approximation coefficients set C and the approximation signal (A). The signal A is constructed by using the set C and has a length of $2^j \times l$ where l is the length of the set C, and this is obtained by the up sampling operation in the DWT (see Fig. 3).

The process that gives rise to the fuel cell RUL prediction can be summarized as follows:

The first step is to construct the prediction model, with the first week (168 hours) being taken as a learning window.

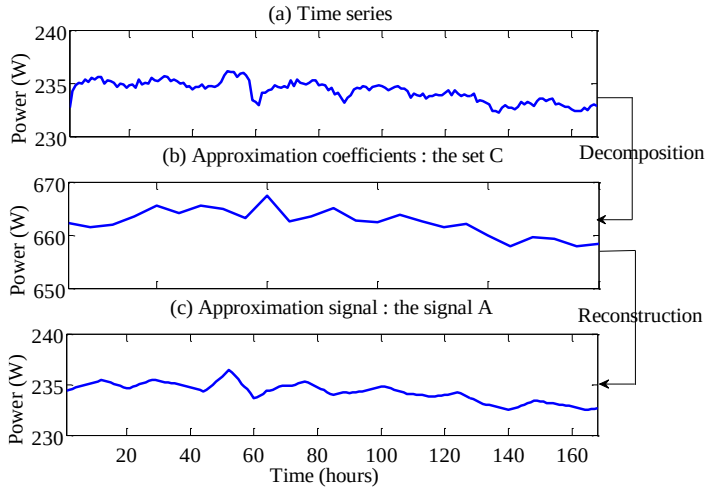

Fig. 3. The approximation coefficients and approximation signal obtained by DWT for a given time series.

The second step is to use this window to perform the prediction for the following week (the following 168 hours). Since in real time the data (or observations) are updated dynamically as the process unfolds, the prediction model uses the second available week (168 hours) to predict the third week (168 hours) and so on, up to 5 weeks.

In order to perform the RUL prediction, four prediction models were used. This allows us to compare the prediction results (first and the second models) and to show the impact of the wavelet transform on the two considered models (the third and the fourth models):

1) First model: A polynomial regression model uses the 168 power signal observations to predict the next 168 hours.

2) Second model: An Auto-Regressive Integrated Moving Average (ARIMA) model functions in the same way as the first model. The ARIMA model, or, more precisely, ARIMA (p,d,q) [41][42] is formulated as follows:

$$y_t = c + \alpha_1 y_{t-1} + \alpha_2 y_{t-2} + \cdots + \alpha_p y_{t-p} + \theta_1 u_{t-1} + \theta_2 u_{t-2} + \cdots + \theta_q u_{t-q} + u_t \quad (4)$$

where y_t is a univariate time series, p is the autoregressive polynomial order, q is the moving average order, $\alpha_1, \alpha_2, \ldots, \alpha_p$ and $\theta_1, \theta_2, \ldots, \theta_q$ are the parameters (or coefficients) of the model, u_t is a white noise.

It should be noted that d in ARIMA(p,d,q) is the differentiation order when the time series is not stationary.

3) Third model: A 3-level DWT using the 'db3' (Daubechie's 3) wavelet (these choices are detailed in section IV) is applied on the learning window; thus, the length *l* of the approximation is $l=168/2^3=21$.

A new polynomial regression model is constructed using these 21 observations, and the model predicts only the next 21 points. Thus, a new set of approximation coefficients D is obtained. D is formed by the old set C plus the 21 prediction points. Thus the length of D is equal to 42.

The approximation signal A is now constructed using the set D. The length of A is $42 \times 2^3 = 336$, which shows that 168 hours are predicted using a prediction of only 21 points. Fig. 4 illustrates this procedure: it shows a set D that contains the set C of Fig. 3. We have the prediction of 21 points, and the reconstruction of the approximation signal A from the set D.

4) Fourth model: An ARIMA model is used to model the set C used in the third model; the set D is obtained by adding the prediction of 21 points to the set C. The prediction also uses an ARIMA model, and is compared with the prediction by the polynomial regression of the third model.

III. Experimental data

As part of the CNRS CO-CONPAC project [43], durability tests are currently being carried out on two similar 600W 5-cell stacks (PEMFCs are assembled at the FCLAB and comprise commercial membranes, diffusion layers and machined flow distribution plates), each cell having an active surface of 100 cm². The first stack FCd is operated under dynamic current operating conditions (ripple current at 5 kHz superimposed on a constant current – peak-to-peak value of 10% of constant current). A second fuel cell stack FCs is operated in stationary regime at more or less nominal conditions over 1000 hours; this second test acts as a reference for the first test. A series of observations are carried out once a week (around every 160 hours) according to the same protocol each time: a polarization curve test, and global historic curves and Electrochemical Impedance Spectroscopy (EIS) measurements.

Relationships between ripple current and fuel cell performance, such as power loss and degradation, are investigated.

The nominal current density of the fuel cells is 0.70 A/cm². Their maximal current density is 1 A/cm². The test bench (Fig. 5) is adapted for PEM fuel cells with a power of up to 1 kW.

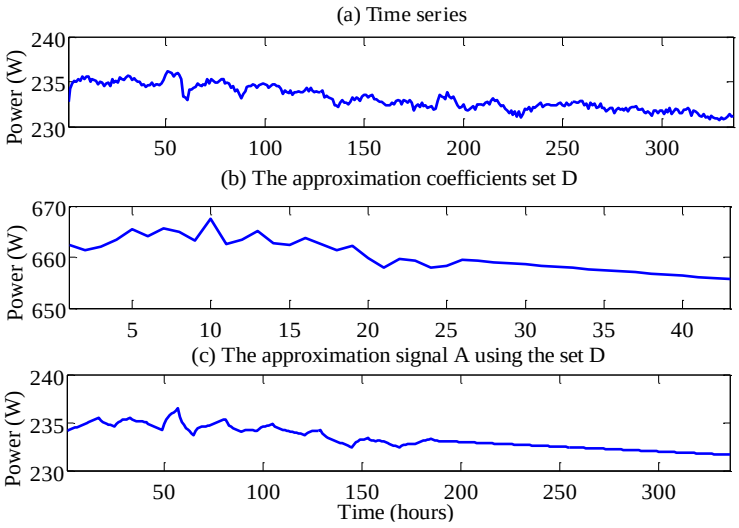

Fig. 4. The approximation coefficients, the set D of predicted coefficients and approximation signal obtained by DWT for a given time series.

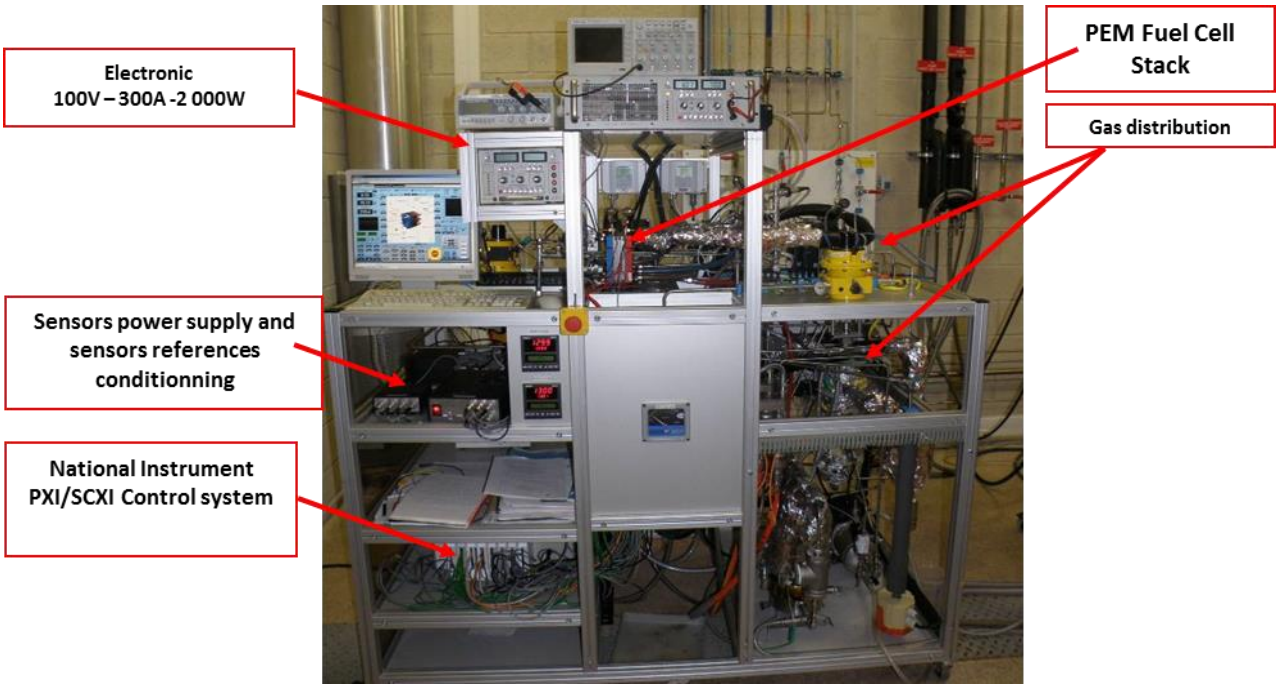

Fig. 5: View of the 1 kW FC test bench.

A number of physical parameters involved in the stack can be controlled and measured in order to create the fuel cells' precise operating conditions as accurately as possible:

- stack temperature, gas flows (from 0 to 100 l/min for air; and from 0 to 30 l/min for H2), fluid hygrometry rates (from 0 to 100%RH), air dew point temperature can be imposed;
- inlet and outlet flows, pressures (from 0 to 2 bars), temperatures (gas temperature from 20°C to 80°C), single cell voltages, stack voltage, current (from 0 to 300 A) can be monitored using a home-made interface developed with Labview™.

Two independent boilers upstream of the stack provide gas humidification. Air and hydrogen go through their respective boilers before reaching the stack. The air boiler is heated in order to obtain the relative humidity desired, while the hydrogen boiler remains at room temperature. The temperature of the cell is controlled by a water-cooling system (with a cooling flow that can be set from 0 to 10L/min and a cooling temperature from 20°C to 80°C).

The current supplied by the battery is controlled by a TDI Dynaload-type active load. For the tests with high frequency ripple current, the load is driven by a low generator frequency. In normal operation, without current disturbance, the charge is conventionally driven from the management interface Labview.

A. Description of the tests carried out

Two long-term tests, each of 1000 hours, were carried out (Fig. 6 and Fig. 7).

1. The ageing test was performed under dynamic condition

The FC stack durability test consists in operating an FC stack with identical characteristics under dynamic current loads and with the time target of 1000 hours. A ripple current of 70A with 7A oscillations at a frequency of 5 kHz was imposed on the FC in order to simulate the global operation effect of the high frequency power converter connected to the output of the FC stack. A complete characterization of the FC was performed every week (around 160 hours) in this order: polarization curve followed by electrochemical impedance spectroscopy (EIS) (the values are the same as for the second test). The characterizations were done at hours: 0, 35, 182, 343, 515, 666, 830, and 1016.

2. The reference ageing test was performed on the second fuel cell stack (FCs). The durability experiment consists in operating the FC stack over 1000 hours in stationary conditions (a current of 70A is imposed). A complete characterization of the FC was performed every week. The duration of the tests was adapted to create the best fit with the first experiment. First, an electrochemical impedance spectroscopy (EIS) was performed only at 70A (0.70 A/cm²), in order to evaluate the state of the FC before it could be modified by the polarization curve. Second, a polarization curve was performed: the stack and cells voltages were measured under a current ramp from 0 A/cm² to 1 A/cm² of 1000s. In order to keep stoichiometric factors constant, the air and hydrogen flows were reduced to a current of 20A. An electrochemical impedance spectroscopy (EIS) was then performed, with measures made in the following order: 70 A (0.70 A/cm²), 45 A (0.45 A/cm²) and 20 A (0.20 A/cm²). Between each measure, a stabilization period of 15 minutes ensured the stability of the parameters. The characterizations were done at hours: 0, 48, 185, 348, 151, 658, 823, and 991.

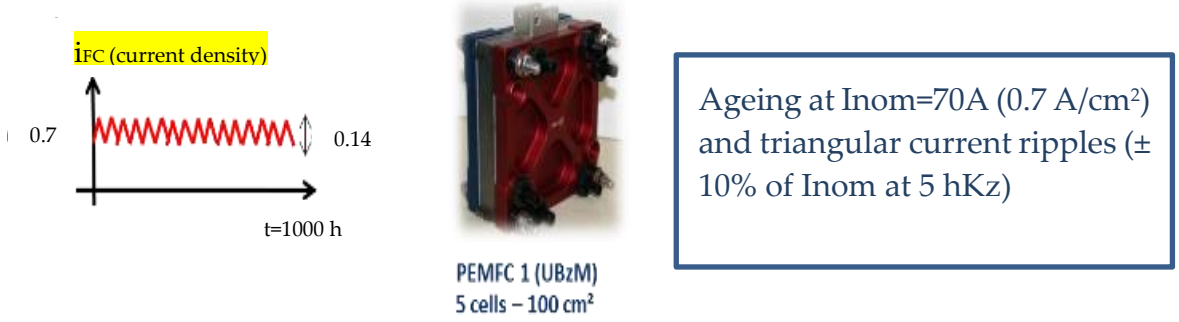

Fig. 6: 1st long-term test (FCd): 1000 h with high-frequency current oscillations

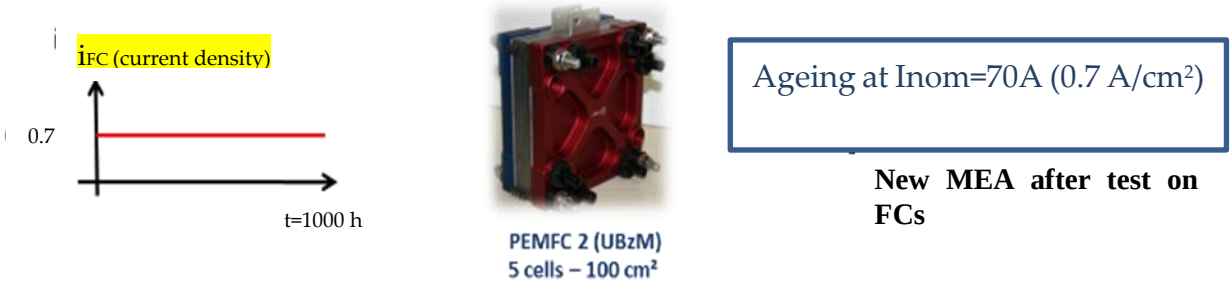

Fig. 7: 2nd long-term test (FCs): 1000 h without current oscillations

B. *Results / Ageing curves*

Temporal curves of the voltage were analyzed in order to estimate the degradation rate. An illustration is given in Fig. 8, which depicts the voltage drop and the corresponding approximation using a least squares method. R^2 (a coefficient of determination between 0 and 1 that reflects how well the regression fits the data - the closer it is to 1, the better the fit) is higher for the second test, as a result of the absence of oscillations and discontinuities as the cells' voltage changes over time.

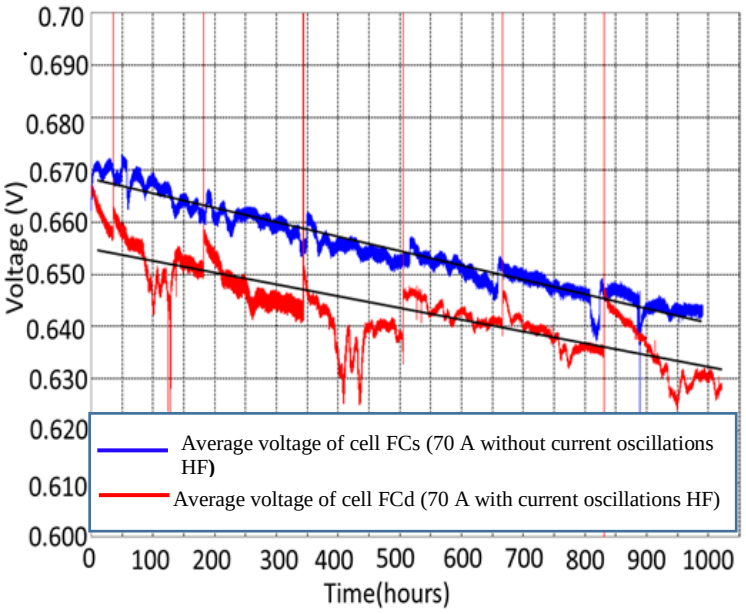

Fig. 8: Comparison of cell average voltage (Red : FCd with current oscillations ; Blue : FCs without current oscillations)

A similar analysis (estimation of the degradation rate) was performed using polarization curves (see Fig. 9 for an illustration). In the two experiments, we can see that the fifth cell presents a higher degradation rate; this is due to its position in the stack.

The experiment was run for around 1000 hours under stationary conditions, and the average stack voltage decay rate was shown to be 153 µV/h per stack and 29.6 µV/h per cell. However, the voltage decay rate observed in dynamic conditions is slightly higher (less than 1% of average voltage) at 172 µV/h per stack and 33.4 µV/h per cell.

In order to implement the proposed approach, a control system was installed based on an Autobox™ (Dspace) using MATLAB/SIMULINK, enabling a direct connection between the model and the system.

IV. Results and discussion

The prediction results corresponding to the different proposed models are presented in Fig. 10 and Fig.11.

Tables (I) and (II) show how the degradations (estimated using the mean values) progressed over time. These degradations are measured with respect to the initial values of the considered power signals.

The online degradation predictions are made as follows: The first week (168 hours) is used to construct and learn the models. The predictions are performed over the following week (the second week). In other words, the prediction horizon is 168 hours.

The models are updated using the new available data for the second week, and the predictions are made over the third week; and so on, up to five weeks.

The model simulations and predictions were done using MATLAB software

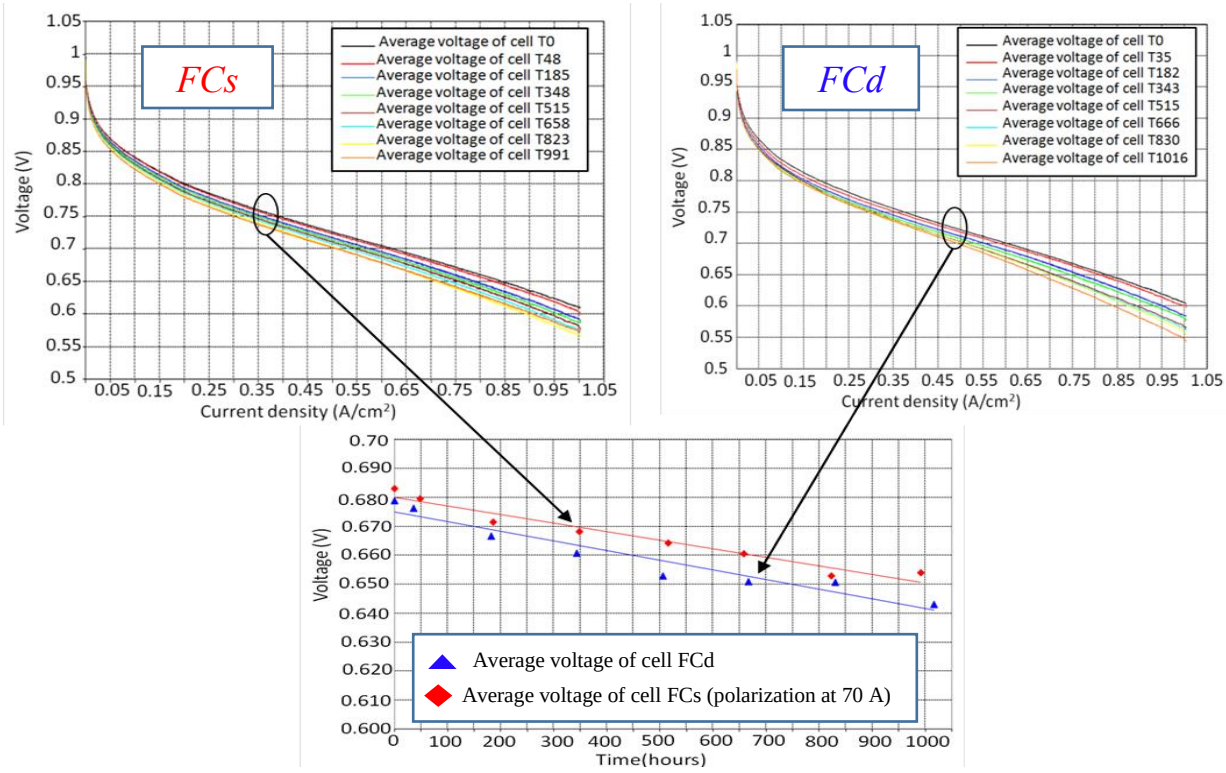

Fig. 9: Comparison of cell average voltage (polarization curves at I=70 A)

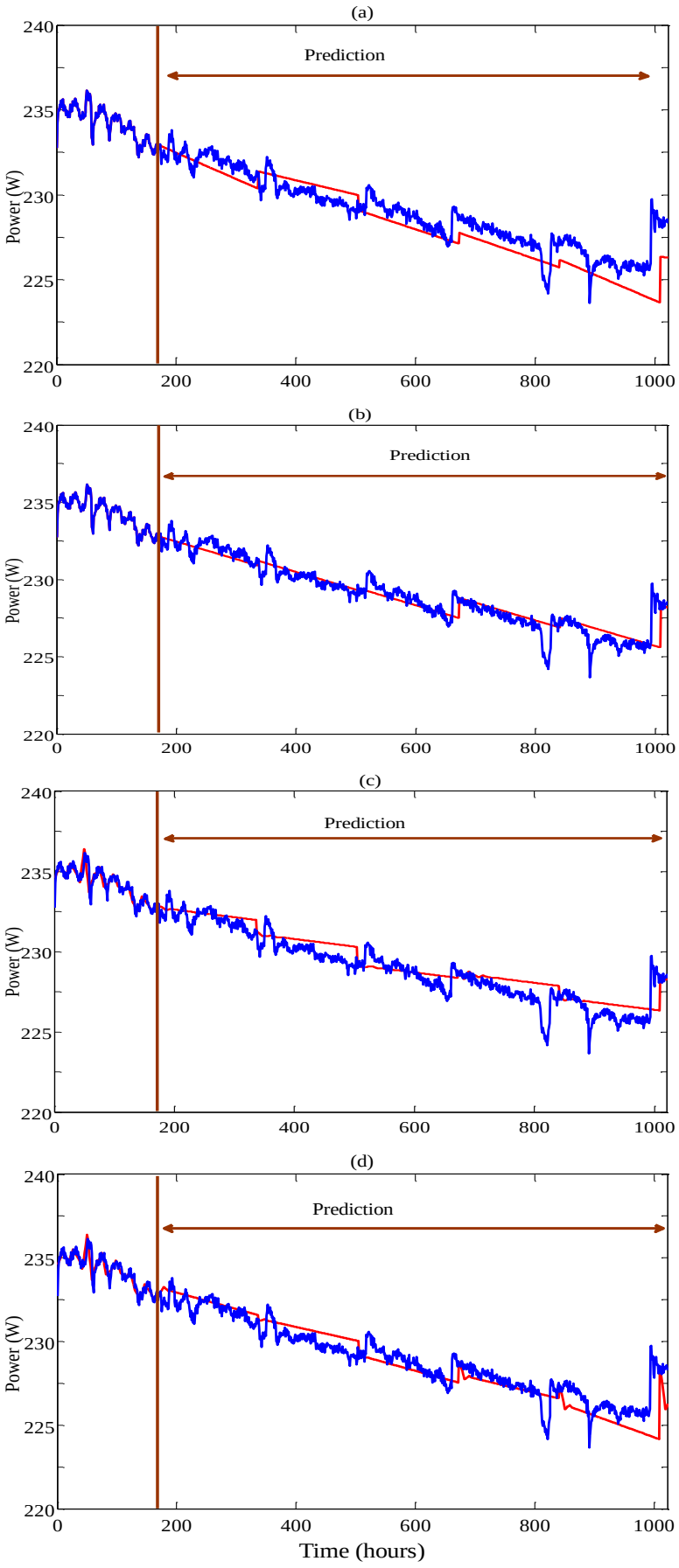

Fig. 10 Prediction results of the power signal for FCs (steady state conditions) applying the first, second third and fourth models in (a), (b), (c) and (d) respectively. The red and the blue lines represent respectively the prediction and the actual signal.

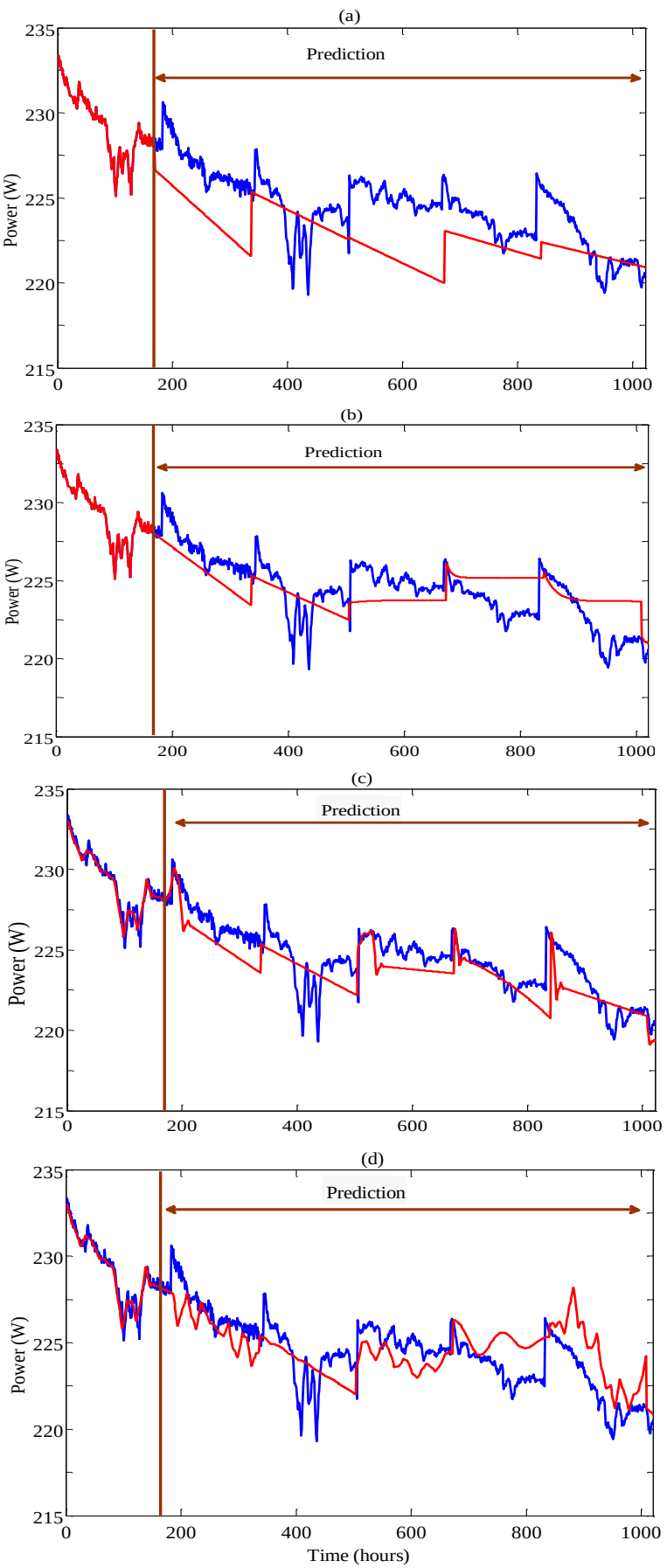

Fig. 11 Prediction results of the power signal for FCd (dynamic conditions) applying the first, second third and fourth models in (a), (b), (c) and (d) respectively. The red and the blue lines represent respectively the prediction and the actual signal

A list of existing programmed MATLAB functions can be found in the econometric and wavelet toolboxes, to be used for time series modelling, prediction and decompositions.

Results are analyzed in the following two paragraphs. The models are compared to show how DWT was able to improve the predictions.

TABLE I
THE MEAN VALUES OF THE ACTUAL AND THE PREDICTED POWERS OVER THE 5 WEEKS FOR THE POWER SIGNAL OF STACK FCs (STEADY STATE CONDITIONS)

	Mean of actual power signal for FCs	Mean of predicted power signal for FCs : first model	Mean of predicted power signal for FCs: second model	Mean of predicted power signal for FCs : third model	Mean of predicted power signal for FCs :fourth model
Week 2	232.1	231.7	231.8	232.4	232.4
Week 3	230.1	230.7	230.2	230.7	230.7
Week 4	228.8	228.1	228.5	228.4	228.8
Week 5	227.4	226.7	227.8	227.3	228.2
Week 6	226.4	224.9	226.5	225.3	226.2

In the first paragraph, models 1 and 3 (without DWT) are compared with models 2 and 4, where the DWT is used (see section II), for the first and second stacks FCs and FCd. In the second paragraph, the results for FCs and FCd are compared.

TABLE II
THE MEAN VALUES OF THE ACTUAL AND THE PREDICTED POWERS OVER THE 5 WEEKS FOR THE POWER SIGNAL OF STACK FCd (DYNAMIC CONDITIONS)

	Mean of actual power signal for FCd	Mean of predicted power signal for FCd: first model	Mean of predicted power signal for FCd: second model	Mean of predicted power signal for FC : third model	Mean of predicted power signal for FCd: fourth model
Week 2	227.0	224.1	225.7	225.9	226.0
Week 3	224.1	223.9	223.9	223.7	223.7
Week 4	225.1	221.3	223.8	224.1	224.0
Week 5	223.7	222.2	225.2	223.0	225.1
Week 6	222.5	221.7	223.9	221.9	224.2

A. Analysis of the results: comparison of the models

In order to compare the prediction results, the first and second models are compared with the third and fourth models respectively.

Regarding the first model (regression without DWT), a polynomial of degree 1 was attributed to the learning window: this polynomial fits the data better than higher polynomial degrees. For the DWT part in the third model, a 3-level decomposition and construction and the Daubechie's 3 wavelet (db3) were used for both the decomposition and the reconstruction operations. These choices are justified as follows:

Since the division of 168 hours (learning part) by 2^3 gives 21 hours, this is the nearest obtained value to 24 hours (one day), so a general trend of the power during one day can be observed. The mother wavelet is db3. Sym3 would give the same results, since db3 and sym3 have exactly the same filter coefficients [36]. Table (III) gives values of the mean square error defined by equation (5) between the approximation and the original signal, for the same level of decomposition using different mother wavelets: Morlet, Coif (Coiflet), Meyer, Sym (Symlet), and Db (Daubechie's). The numbers in the wavelets Coif2, 3, 4 and 5, Sym 2, 3, 4 and 5 and Db2, 3, 4, and 5 correspond to the numbers of terms of the corresponding wavelet [40]. The values in table III represent the errors (obtained using equation (5)) between the signal of approximation (reconstructed using the approximation coefficients) and the original signal. These values are provided in order to help finding the best wavelet to perform the algorithm. The wavelet that gives the smallest error, is the then chosen.

$$E = \frac{1}{N}\sum_{i=1}^{N}(P(t) - a_t)^2 \quad (5)$$

where N is the length of the approximation signal of level 3, a_t is the t[th] approximation signal and $P(t)$ is the actual power.

TABLE III
COMPARISON OF THE MEAN SQUARE ERRORS USING DIFFERENT MOTHER WAVELETS

	FCd	FCs
Db2 (or sym2)	0.1402	0.1228
Db3(or sym3)	0.1156	0.0936
Db4(or sym4)	0.1235	0.1131
Db5(or sym5)	0.1315	0.1130
Coif2	0.1252	0.0983
Coif3	0.1357	0.116
Coif4	0.1184	0.1067
Coif5	0.1327	0.1091
Dmey	0.1273	0.1024

The chosen wavelet is the one gives the smallest error for the approximation signal, which is db3.

In Fig. 10(a) and 10(c), it can be seen that for the third model, the predictions are closer to the actual observations. Although they do not have exactly the same variations of the original signals, their behavior can nevertheless correspond: for much of the time they can approximate the mean value of the signals, and occasionally be very similar to them (see table I), which can provide solid indications about processes of degradation.
Table (IV) shows the prediction errors.

The error used in this study is the relative error having the formulations:

$$RMSE(e) = \sqrt{\frac{\sum_{t=1}^{n}\left(P(t)-\hat{P}(t)\right)^2}{n}} \quad (6)$$

and

$$\max(e) = max\left|\frac{P(t)-\hat{P}(t)}{P(t)}\right| \quad (7)$$

where $\hat{P}(t)$ is the prediction of P at time t.

Tables IV to VI show that the predictions made using the third model have the fewest errors.
Regarding the comparison between the second and the fourth models:
The ARIMA models that best fit the observations are ARIMA(5,1,0), ARIMA(5,0,1) and ARIMA(5,0,0). The model

updates its coefficients when new actual values of a new week are made available.

TABLE IV
COMPARISON OF PREDICTION ERRORS (UNIT W) BETWEEN DIFFERENT METHODS FOR SIGNALS IN STEADY STATE CONDITIONS

	RMSE of predicted power signal for FCs : first model	RMSE of predicted power signal for FCs: second model	RMSE of predicted power signal for FCs : third model	RMSE of predicted power signal for FCs: fourth model
Week 2	0.7	0.6	0.5	0.5
Week 3	0.8	0.8	0.8	0.4
Week 4	0.8	0.6	0.7	0.6
Week 5	0.9	1.1	0.7	0.7
Week 6	1.9	1.1	1.6	1.1

As shown in Fig. 10(b) and 10(d), DWT can improve the prediction for the ARIMA models. Table (I) shows that the predictions can also approximate the mean of the actual observations, and in table (IV) the comparison of errors proves again that DWT improves the quality of prediction. The comparisons of models for the stack FCd (dynamic conditions) can be seen in Fig.11, and in tables (II) and (VI).

For Fig.11 (a), the polynomial regression fails to capture the general behaviors of the degradations obtained by the first model. However, Fig. 11(c) shows the improvement obtained when DWT is added to the polynomial regression (third model); here the polynomial is of degree 2. It can clearly be seen that with DWT the model captures the process of degradation. Tables (I) and (IV) give numerically the impact of DWT in reducing the prediction errors.

Here too, the impact of DWT is demonstrated. The situation for Fig. 11(b) (second model) and Fig. 11(d) (fourth model) is similar: DWT is seen to improve the prediction with the ARIMA model.

Finally, as shown in tables (I) to (VI),the errors obtained by the ARIMA-DWT model are less than the regression-DWT, showing thus that this is the best model (among the four models considered in this paper) to implement a prognostic strategy for a fuel cell.

TABLE V
COMPARISON OF PREDICTION ERRORS (UNIT W) BETWEEN DIFFERENT METHODS FOR SIGNALS IN DYNAMIC CONDITION

	RMSE of predicted power signal for FCd : first model	RMSE of predicted power signal for FCd: second model	RMSE of predicted power signal for FCd : third model	RMSE of predicted power signal for FCd: fourth model
Week 2	3.0	1.5	1.4	1.3
Week 3	1.5	1.5	1.6	1.6
Week 4	3.8	1.5	1.2	1.2
Week 5	1.7	1.8	1.3	1.8
Week 6	1.6	2.1	1.3	1.9

B. Analysis of the results: comparison of the stacks

The main difference between stacks FCs and FCd is that stack FCd is subjected to dynamic operating conditions (see section II) that affect the prediction results.

Let us now look at Fig. 10(d) and 11(d). In the case of stack FCs, the model shows more stability in approximating the observations. But this is to be expected, since the trend of the voltage signal of FCd (see Fig. 8) drops linearly and no ripple variations are added to this stack; while the trend of the voltage for FCs is variable, since dynamic ripples are added to the stack.

TABLE VI
COMPARISON OF MAXIMUM PREDICTION ERRORS (AMONG FIVE WEEKS, YSING EQUATION (7)) BETWEEN DIFFERENT METHODS FOR SIGNALS IN STEADY STATE AND DYNAMIC CONDITIONS

	Regression with DWT	Regression without DWT	ARIMA with DWT	ARIMA without DWT
Power signal of A	2. 36 %	2.57 %	1.69 %	1.75 %
Power signal of B	2.40 %	2. 81 %	1.97%	2.03%

Nevertheless, the predictions can be considered as acceptable for both stacks, according to the small percentage errors given in table (VI).

C. RUL Estimation:

Since the best prediction results are obtained using the fourth model, the RUL is estimated according to this model. A flowchart of the algorithm represented by the fourth model can be found in Fig. 12. In this work the RUL is defined as the time (in hours) until power drops by 5.5% in relation to its initial value.

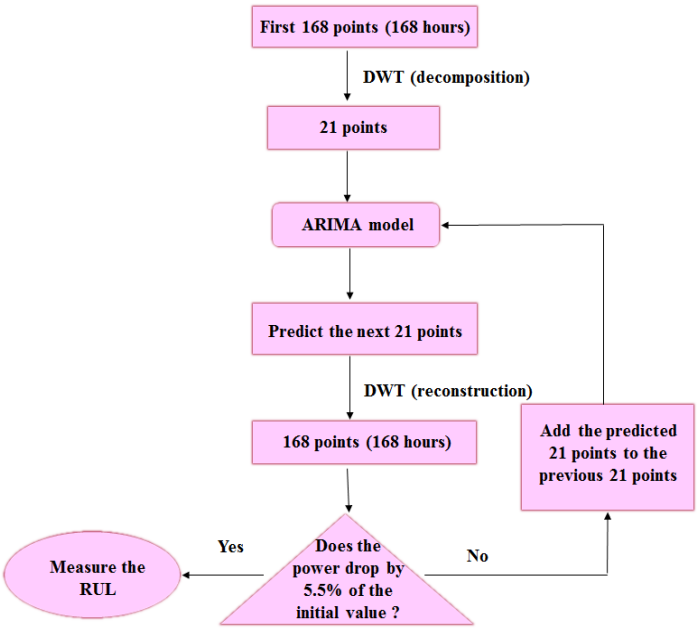

Fig. 12 A flowchart of the fourth model.

Fig.13 (a) shows the results for stack FCs. As the initial value of the power is about 236 W, the actual RUL is about 811 hours, corresponding to a drop of 5.5% to ~223 W (end of the fifth week). Using model 4, the predicted (or estimated) RUL for the same stack is 893 hours (beginning of the sixth week), which represents a difference of ~82 hours between the estimation and the actual RUL.

As for the stack FCd, the results are presented in Fig. 13(b). The initial value of the power is also about 236 W and after a drop of 5.5% it is therefore about 223 W, indicating an actual RUL of about 400 hours (the third week). The RUL estimated using the fourth model was found to be 469 hours (also in the third week).

We conclude that model 4 can give a quite robust estimation of the RUL, close to the real figure, for both stacks under different operating conditions, static and dynamic.

D. Discussions

The obtained results are very promising. A number of strong points of the proposed method can be summarized as follows:

- Its rapid execution time for both the learning and the prediction parts (an estimation of the order of seconds) makes it superior to other data-driven algorithm, that is to say artificial neural network algorithms that have a high time cost.
- It has no training part and thus does not include any black box systems that are often difficult to adapt to any change in data. Instead, it uses analytical equations.

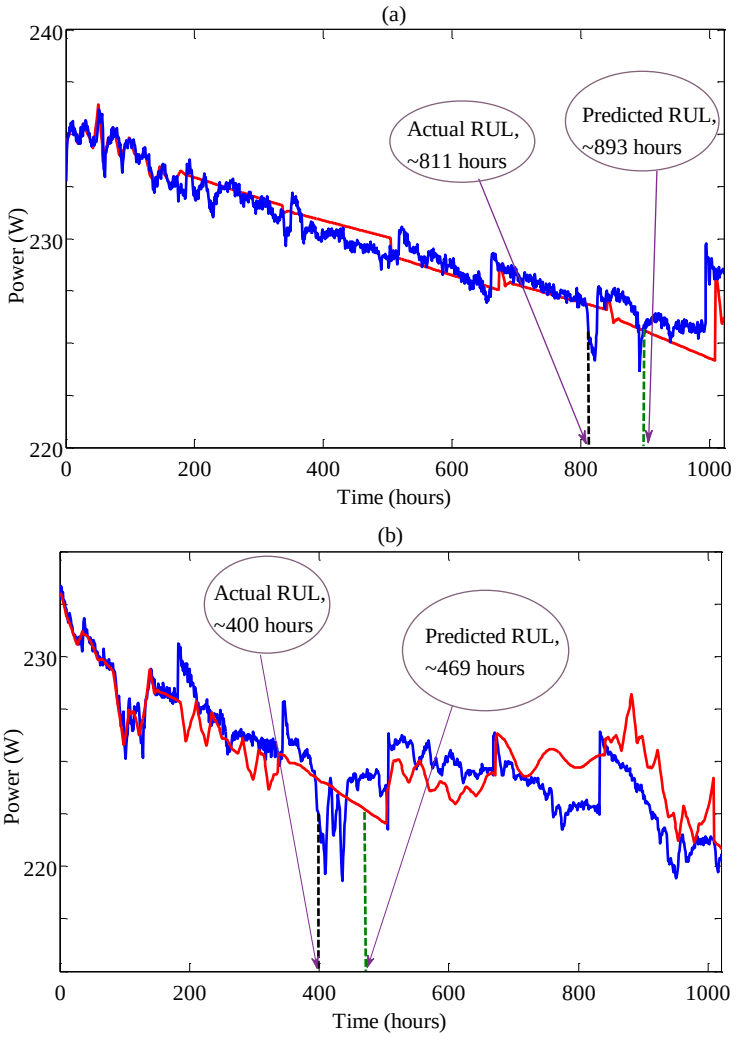

Fig. 13 (a) RUL prediction of the stack FCs using the fourth model, and (b) RUL prediction of the stack FCd using the fourth model. The red line correspond to the prediction and the blue line corresponds to the actual signal

- The model requires fewer data (only 168 observations) for learning, and no exogenous data are needed to perform the prediction for both stacks. A reduced reliance on measurement devices, means reduced instrumentation cost and reduced testing time.
- It provides a close approximation of the actual observations, as shown in table (VI) (no more than 2.81% error). Moreover, it is clear that, even under dynamic operations, the predictions include variations that are similar to the actual variations (Fig. 11(d)).
- The model is able to estimate RUL, since the power decrease has direct impact on the RUL. In the case of the stacks considered in this work, the RUL is estimated as the time until the power drops by 5.5%.

The proposed model could nevertheless be improved by adding some degradation factors such as the use of materials and the occurrence of drying and flooding faults in the fuel cell: these two faults occur successively inside the fuel cell and have negative impact on the performance of the cell [44], leading to drops in the power signals, indicating a loss of fuel cell efficiency.

V. Conclusion

An approach based on DWT for estimating the RUL for a stack of PEMFCs is presented in this paper. The novelty of the presented techniques is the use of DWT for estimating the RUL, and the use of univariate models without training. The main advantage, in comparison to similar works on this topic, is the time series domain analysis that uses past information from a univariate time series (the power signal). Its reliance on measurement devices and on data are therefore reduced. This approach can be used for general cases, since the mathematical models do not take into account the variations that are to be found in exogenous data, under different operating conditions. It can be coded easily in any computer language, and thus easily implemented in real life applications.

The proposed method was simulated in MATLAB/SIMULINK, and compared with other models; the results showed that with DWT, the prediction is more accurate and faster.

It may be interesting to compare the DWT with other filters, such as unscented particle filters and adaptive neuro-fuzzy inference systems that have also been used for estimating RUL in electrochemical batteries.

References

[1] H. Ramirez-Murillo, C. Restrepo, J. Calvente, A.Romero, R. Giral, "Energy management of a fuel cell serial-parallel hybrid system", *IEEE Trans. Ind. Electron* , DOI 10.1109/. 2015.2395386, 2015

[2] F.Barbir, PEM Fuel Cells: Theory and Practice, Academic Press, 2013.

[3] H.Ibrahim, A.Ilinca, J.Perron, "Energy storage system-characteristics and comparisons", *Renewable and Sustainable Energy Reviews*, vol. 12, n. 5, pp. 1221-1250, 2008.

[4] C.De Beer, P.S.Barendsa, P.Prillay, "Fuel cell condition monitoring using optimized broad band impedance spectroscopy", *IEEE Trans. Ind. Electron* . DOI 10.1109/ 2015.2418313, pp. 1-11, 2015.

[5] Z.Li, R.Outbib, D.Hissel, S.Giurgea, ''Diagnosis for PEMFC systems: a data-driven approach with the capabilities of online adaptation and novel fault detection'', *IEEE Trans. Ind. Electron*, DOI: 10.1109/TIE.2015.2418324, pp. 1-11, April 2015

[6] C.Kunusch, C.Ocampo-Mrtinez, M.Valla,, modeling , diagnosis and control of fuel-cell-based technologies and theur integrations in smart-grids and automotive systems, *IEEE Trans. Ind. Electron*.,n.99, DOI. 10.1109/TIE 2015.2440212, pp. 1-3, Jun 2015

[7] D.Debanjak, J.Petrovcic, P.Boskoski, B.Musizza, D. Juricic, "Fuel cell condition monitoring system based on interconnected DC-DC converter and voltage monitoring", *IEEE Trans. Ind. Electron*., DOI. 10.1109/TIE. 2015.2434792, pp.1-12, 2015,

[8] M.Yu, D.Wang, M.Luo, "An integrated approach to prognosis of hybrid systems with unknown mode changes", *IEEE Trans. Ind. Electron*., vol 62, no.1, pp. 503-515, Jan .2015.

[9] E. Lechartier, R. Gouriveau, M.-C. Pera, D. Hissel, and N. Zerhouni, 2014, Static and dynamic modeling of a PEMFC for prognostics purpose, in Vehicle Power and Propulsion Conference (VPPC) 2014, pp. 1–5.

[10] Y.B. Zhang, Y.X. Jia, X.M. song, Q.Gu, A RUL model based on KICA and maximum likelihood estimation with particle filters, International Conference on Quality, Reliability, Risk, Maintenance and Safety Engineering (ICQR2MSE) June 2011, pp. 527-531

[11] A.Ray, S.Tangirala, 1997, “A nonlinear stochastic model of fatigue crack dynamics”, Probabilistics Engeneering Mechanics, vol 12, no. 1, pp. 33-40, 1997

[12] R.W. Swindeman, M.J. Swindeman, “A comparison of creep models for nickel base alloy for advanced energy systems”, *International Journal of Pressure Vessels and Piping*, vol. 85, no. 1-2, pp. 72-79, 2008.

[13] P.Baraldi, F.Cadini, F. Mangili and E. Ziao, “Model-based and data driven prognostics under different available information”, *Probabilistics Engineering Mechanics*, vol. 32, pp. 66-79, 2013.

[14] R.K.Singleton, E.G. Strangas, S.Aviyente, “Extended Kalman Filtering for remaining useful life estimation of bearings”, *IEEE Trans. Ind. Electron*, vol 62, no.3, pp. 1781-1790, Jan 2015.

[15] L.Peel, “Data driven prognostics using a Kalman filter ensemble of neural network models”, 2008, Proceeding of the int.conf.on prong. And health manag., 2008

[16] A. Soualhi, H.Razik, G.Clerc, D.D.Doan, “Prognosis of bearing failures using Markov models, and the adaptive neuro-fuzzy interface systems”, *IEEE Trans. Ind. Electron*., vol 61, n.6, pp. 2864-2874, Jun. 2014

[17] R. Silva, R. Gouriveau, S. Jemei, D. Hissel, L. Boulon, K. Agbossou, N. Y. Steiner, 2014, “Proton exchange membrane fuel cell degradation prediction based on adaptive neuro-fuzzy inference systems”, *International Journal of Hydrogen Energy*, vol. 39, no. 21, pp. 11 128–11 144.

[18] N.Laayouj, H.Jamouli, “Remaining useful life prediction of lithium-ion battery degradation for a hybrid electric vehicle”, Global Advanced *Research Journal of Engineering, Technology and Innovation*, vol. 4, no. 2, pp. 016–023, 2015.

[19] Y.Hu, P.Luo, “Performance data prognostics based on relevance vector machine and particle filter”, *Chemical Engineering Transactions*, vol. 33, pp. 349–354, 2013.

[20] H.Li, C.L.Philip Chen, “Intelligent prognostics for battery health monitoring using the mean entropy and relevance vector machine”, *IEEE Trans. Sys. Man. Cybern. Sys*. , vol 44, no. 7, pp. 851-862. Jul. 2014

[21] L.Liao, “Discovering prognostic features using genetic programming in remaining useful life prediction”, *IEEE Trans. Ind. Electron*., vol 61, n.5, pp. 2464-2472,May 2014

[22] M.Jouin, R.Gouriveau, D.Hissel, M-C. Pera, N. Zerhouni, “Prognostics and health management of PEMFC-State of the art and remaining challenges”, *International Journal of Hydrogen Energy*, vol. 38, no. 35, pp. 15307–15317., 2013.

[23] K.Javed, R. Gouriveau, N.Zerhouni and D.Hissel, Data-driven prognostics of proton exchange membrane fuel cell stack with constraints based summation-Wavelet extreme learning machine, FDFC2015.

[24] S. Morando, S. Jemei, R. Gouriveau, N. Zerhouni, D. Hissel, 2013, Fuel cells prognostics using echo state network, in Industrial Electronics Society, IECON 2013-39th Annual Conference of the IEEE, pp. 1632–1637.

[25] M.Jouin, R.Gouriveau, D.Hissel, M-C. Pera, N. Zerhouni, “Prognostics of PEM fuel cell in a particle filtering framework”, *International Journal of Hydrogen Energy*, vol. 9, no. 1, pp. 481–494. 2014.

[26] K.Javed, R. Gouriveau, N.Zerhouni P. Nectoux, Enabling health monitoring approach based on vibration data for accurate prognostics, *IEEE Trans. Ind. Electron*., vol 62, n.1 pp.647-656, Jan 2015

[27] D. Beniouioua, D. Candusso, F. Harel, L. Oukhellou, PEMFC stack voltage singularitiy measument and fault classification, *International journal of hydrogen energy*, vol. 39, pp. 21631-21637, December 2014

[28] A. Debenjak, P. Boskoski, B. Misizza, J. Petrovcic, D. Juricic, Fast measurement of proton exchange membrane fuel cell impedance based on pseudo-random binary sequence perturbation signals and continuous wavelet transform, *Journal of Power Sources*, vol. 254, pp:112-118, 2014.

[29] M. Ibrahim, U. Antonyi, N.Y. Steiner, S. Jemei, C. Cokonendji, B. Ludwig, P. Moçotoguy, D. Hissel, Signal-based diagnosis by wavelet transform for proton exchange membrane fuel cell, *Enegry Procedia*, vol. 74, pp. 1508-1518, August 2015

[30] N. Y. Steiner, D. Hissel, P. Moçotéguy, D. Candusso, Non-intrusive diagnosis of polymer elecltrolyte fuel cells by wavelet packet transform, *International journal of hydrogen energy*, vol. 36, pp. 740-746, 2011

[31]Y. Ren, Z.D. Zhong, T.Y. Luo, A combined particle swarm optimization-wavelet transform based strategy for power management of PEM fuel cell powered hybrid system, *Advanced Materials Research*, vols. 971-973, pp. 954-957, June 2014

[32] K. Javed, R. Gouriveau, N. Zerhouni, D. Hissel, Improving accuracy of long-term prognostics of PEMFC stack to estimare remaining useful life, IEEE international conference on industrial technology (ICIT), March 2015, pp. 1047-1052

[33] A. Bouzida; O. Touhami; R. Ibtiouen; A. Belouchrani; M. Fadel; and A. Rezzoug, “Fault diagnosis in industrial induction machines through discrete wavelet transform. *IEEE Trans. on Indust. Electron.* , Vol.58, N°9, 2011, pp.4385-4395

[34] K. Lakshmi Varaha Iyer; Xiaomin Lu; Yasir Usama; Vamsi Ramakrishnan; and Narayan C. Kar, “A twofold debauchies-wavelet-based module for fault detection and voltage regulation in SEIGs for distributed wind power generation. *IEEE Trans. on Ind. Electron.*, Vol.60, N°4, 2013, pp.1638-1651

[35] Bialasiewicz, J.T.; Gonzalez, D.; Balcells, J.; Gago, J., “Wavelet-Based Approach to Evaluation of Signal Integrity*” IEEE Trans. on Ind. Electron.* Vol.60, N°10, 2013, pp.4590-4598

[36] M. Misiti, Y.Misiti, G. Oppenheim and J.M. Poggi, Wavelets and their applications, ISTE Ltd, 2010.

[37] T.M.Rauber, F.de Assi Boldt, F.M. Varejao, “Heterogeneous features models and feature selection applied to bearing fault diagnosis”, *IEEE Trans. Ind. Electron.*, vol 62, n.1, pp. 637-646, Jan 2015.

[38] K.Zhu, T.Mei, D.Ye,Online condition monitoring in micro milling: a force waveform shape analysis appraoch, *IEEE Trans. Ind. Electron*., vol 62, n.6, pp.3806-3813, Jun 2015

[39] Y. Sheng, Wavelet Transform, the wavelet transforms and applications handbook, second edition, Press LLC, 2000.

[40] S. Mallat, A wavelet tour of signal processing: the sparse way, third edition: Academic Press, 2008.

[41] M.Ibrahim, G.Wimmer, S.Jemei and D.Hissel, Energy management for a fuel cell hybrid electric vehicle, 40th Annual Conference of the IEEE Industrial Electronics Society, IECON2014.

[42]G.Box, G.Jenkins, G.Reinsel, Time series analysis: forecasting and control, 14th edition, Wiley, 2008

[43], B.Wadhame, L.Girardot, D.Hissel,F.Harel, X . Francois, D.Candusso, M.C. Péra, L. Dumercy, “Impact of power converter current ripple on the durability of a fuel cell stack”, IEEE ISIE'08 International Symposium on Industrial Electronics, CD-ROM, pp. 1495-1500, Cambridge, UK, 2008.

[44] M.Gerard, J.-P. Poirot-Crouvezier, D.Hissel, M.-C. Pera, “Ripple current effects on pemfc aging test by experimental and modeling”, *Journal of Fuel Cell Science Technology*, vol.8, n.2, pp. 1-5, 2011.